JOURNAL OF CATALYSIS 135, 400–419 (1992)

Mechanistic Aspects of the Higher Alcohol Synthesis over K_2O-Promoted ZnCr Oxide: Temperature-Programmed Reaction and Flow Experiments of C_3, C_4, and C_5 Oxygenates

LUCA LIETTI, ENRICO TRONCONI, AND PIO FORZATTI

Dipartimento di Chimica Industriale ed Ingegneria Chimica "G. Natta" del Politecnico, Piazza Leonardo da Vinci 32, 20133 Milano, Italy

Received June 19, 1991; revised December 19, 1991

Mechanistic aspects of the higher alcohol synthesis (HAS) over a K_2O-promoted ZnCrO catalyst are investigated by temperature-programmed surface reaction (TPSR) of C_3 oxygenates (1-propanol, *n*-propanal, and *n*-propanoic acid) and by flow microreactor experiments of 1-propanol, 3-pentanone, and 2-butanone. A number of chemical functions are identified by the TPSR study, including hydrogenation–dehydrogenation, "normal" and "reversal" aldolic-type condensations, ketonizations, "reversal" α-addition, dehydration, decarboxylation, and cracking. On comparing the data with those obtained during flow experiments over the same catalyst, a strict correspondence is observed between the chemical functions indicated by the TPSR study and those prevailing under steady-state conditions. However, under these conditions some of the associated chemical reactions (namely hydrogenation and ketonization) appear to be limited by chemical equilibrium and the peculiar reactivity of the different species participating in the reactions is appreciated. TPSR and continuous-flow experiments lead to the identification of a general reaction network for C_N oxygenate molecules, based on the following routes; (i) hydrogenation/dehydrogenation reactions of oxygenate molecules; (ii) aldolic-type condensations of aldehydes and ketones, both in the normal and in the reversal mode, leading to the formation of higher aldehydes and ketones; (iii) ketonization reactions, leading to the formation of ketones and CO_2; (iv) reversal α-addition reactions, which result in the formation of 2-ketones; (v) dehydration of oxygenates, and particularly of secondary alcohols, leading to the formation of olefins. Olefins may also be formed by decarboxylation of surface carboxylate species. The reactivity of the species participating in the various reactions is discussed on the basis of their molecular structure, and results are compared with catalytic tests performed under HAS conditions. It is found that the reaction pattern identified in the present study basically describes the data collected under pressure.

INTRODUCTION

It is well known that the synthesis of methanol and higher alcohols from carbon monoxide and hydrogen (higher alcohol synthesis, HAS) is effectively catalized by alkali-promoted high-*T* and low-*T* methanol synthesis catalysts (*1–11*). The origin of C_{2+} oxygenates over modified low-*T* Cu-based catalysts has been recently clarified by Klier and co-workers (*5, 12–14*) and by Elliott and Pennella (*15–18*). Mechanistic aspects of the HAS over modified high-*T* methanol catalysts were investigated in the early literature (*19–23*). More recently the mechanism of the HAS over unpromoted and K_2O-promoted ZnCrO has been investigated by temperature-programmed surface reaction (TPSR) (*24–27*) and by diffuse reflectance FT–IR spectroscopy (DRIFT) (*28*) of linear and branched C_4 oxygenate molecules (alcohol, aldehyde, and acid). The reaction products formed during TPSR experiments have been explained by invoking the presence of C_4 and C_8 surface intermediate species (alkoxide, aldehyde, and carboxylate). The existence of these species and their stability with temperature have been confirmed by DRIFT experiments. The results indicated that aldolic-type condensations (also with

0021-9517/92 $5.00

oxygen retention reversal), hydrogenation–dehydrogenation, dehydration, decarboxylation, and decarboxylative condensation reactions are effectively catalyzed by ZnCr oxide. TPSR experiments performed over K_2O-promoted ZnCrO further indicated that upon alkali addition the dehydration and decarboxylation functions are reduced, aldolic-type condensations are not significantly affected, and decarboxylative condensations are markedly enhanced.

The comparison of TPSR results and experiments performed under HAS conditions showed that a strict correspondence exists between the major catalyst functions revealed by TPSR and those operating under synthesis conditions. Thus the TPSR technique has proved itself a powerful tool for obtaining direct information on the reaction mechanism operating in the HAS and on the nature of the intermediate surface species involved in the HAS. The same catalyst functions were reported to operate over alkali-promoted low-*T* methanol synthesis catalysts as well (*5, 12, 15, 17*) so that the chemistry involved in the HAS over low-*T* and high-*T* modified methanol catalysts seems to be basically the same. Indeed, the differences between the two types of catalysts concerning the relative amounts of some classes of oxygenated products are readily explained by considering the influence of the different reaction temperature on the chemical equilibria prevailing in the HAS (*30*).

In the present study the TPSR investigation over K_2O-promoted ZnCrO catalyst has been extended to C_3 oxygenates, namely 1-propanol, *n*-propanal, and *n*-propanoic acid. The TPSR study of C_3 oxygenate molecules was designed to provide information on the reactivity of C_3 molecules as compared to C_4 species and eventually to confirm and generalize the catalyst functions previously assessed in the case of C_4 molecules. In this work continuous-flow experiments of 1-propanol at atmospheric pressure have also been performed to obtain data under steady-state conditions. Finally, since ketones were produced in significant amounts, flow experiments were also performed with 3-pentanone and 2-butanone as reagents. All of these data, together with previous data obtained either at atmospheric pressure or under actual synthesis conditions, are discussed with the purpose of identifying the reaction network of C_N oxygenates in the HAS and to differentiate the reactivities of the different oxygenates.

METHODS

The K_2O-promoted ZnCrO catalyst (3% K_2O w/w) was prepared by the incipient wetness impregnation method starting from a commercial ZnCrO system (Zn/Cr atomic ratio = 3/1, BET surface area = 120 m^2/g, phases identified by XRD ZnO and $ZnCr_2O_4$) and using a CH_3COOK solution.

Continuous-flow experiments at atmospheric pressure were performed in a quartz tubular fixed-bed microreactor (i.d. 7 mm). Gas-flow rates were controlled by Brooks mass flowmeter/controllers; liquid reagents were admitted to the reactor through a dedicated heated line by means of a saturator held at constant temperature. In a typical experiment, 160 mg of catalyst were loaded into the reactor and prereduced *in situ* at 450°C for 30 min with He + 80% H_2. Then the catalyst temperature was set to the desired value and the liquid reagents were fed to the reactor. The total gas-flow rate was 100 Ncc/min of He + 80% H_2 and the liquid reagents were fed to the reactor at a rate of 0.8–1.0 μl/min. The analysis of the reaction products was performed by on-line gas chromatography using three columns in a parallel arrangement: an OV1 25-m-long capillary column (0.32 mm i.d.) with high phase thickness (3 μm) connected to a F.I. detector for analysis of hydrocarbons and oxygenates, a packed Porapak column (i.d. 5 mm, L = 4 m) operating at 120°C and connected to a T.C. detector for the analysis of CO_2 and H_2O, and a packed 5-Å molecular sieve column (i.d. 3 mm, L = 1 m) operating at room temperature for analysis of CO.

TPSR experiments were performed in the same apparatus used for catalytic activity runs. The catalyst (160 mg, 120–200 mesh) was reduced with H_2 + 20% He at 450°C for 30 min, heated in He at 470°C to remove physisorbed hydrogen, cooled to 35°C, and saturated with pulses of the adsorbate. Then the catalyst temperature was increased linearly (β = 10.5°C/min) in flowing He (Q = 60 cc/min) up to 470°C and the desorption spectra were recorded. The experimental procedure of TPSR runs was described in detail elsewhere (*25*). For the present study the analysis section of the TPSR apparatus was enhanced by splitting the gases exiting the reactor into two streams: one entering a multiple-loop gas sampling valve (Valco), which allowed several on-line GC analyses of the product mixture, and the other being connected to a quadrupole mass detector QMD (UTI 100 C) coupled with an IBM AT Personal Computer, which scanned the 1-110 AMU range at 10 AMU/s. The above arrangement allowed simultaneous on-line GC and QMD analyses of the reaction products. The identification of reaction products was based on GC retention times and on GC–MS analysis of the liquid product obtained by condensation of the gases exiting the reactor in a liquid nitrogen-cooled trap containing few microliters of CS_2 and located immediately downstream of the reactor (*25*).

The desorption profiles of the single species were obtained as detailed in the following. For each product identified by GC analyses, a characteristic mass fragment was selected and the corresponding QMD profile was chosen to represent its evolution with temperature. Then, on the basis of on-line GC analyses performed at various temperatures, the QMD profiles were scaled in order to reflect the effective product composition of the gases exiting the reactor. When different species with the same characteristic mass fragment desorbed simultaneously, this procedure was not attempted and the desorption spectra were obtained by staged interpolation of the discrete experimental points provided by on-line GC analysis using cubic spline functions.

Chromatographic helium and hydrogen and Aldrich Chemicals ppa 1-propanol, *n*-propanal, *n*-propanoic acid, 3-pentanone, and 2-butanone reagents were used.

RESULTS

1-Propanol TPSR

The overall 1-propanol FID–TPSR trace and the desorption profiles of the single products from K_2O-promoted ZnCrO are presented in Fig. 1. The overall trace consists of a low-temperature peak (T_M = 120°C) associated with 1-propanol evolution and in a high-temperature peak (T_M = 425°C), which originates from desorption of propylene (T_M = 421°C), 3-pentanone (T_M = 420°C), 2-butanone (T_M = 420°C), methane (T_M = 448°C), ethylene (T_M = 428°C), butenes (T_M = 400°C), benzene (426°C), and toluene (412°C). Figure 1 also reports the desorption of hydrogen (T_M = 216 and 414°C), CO (T_M = 435°C), CO_2 (T_M = 437°C), and water (which extends over the whole T-range).

n-Propanal TPSR

Figures 2A and 2B show the overall FID–TPSR trace and the profiles of the main desorbed species upon adsorption of *n*-propanal on K_2O-promoted ZnCrO. Three main peaks are evident in the overall trace: (i) a low-temperature peak with maximum at T_M = 78°C associated with the desorption of the parent molecule (*n*-propanal, T_M = 78°C), 2-methyl-2-pentenal (T_M = 82°C), 1-propanol (T_M = 85°C), and 3-pentanone (T_M = 78°C); (ii) a peak with maximum at T_M = 250°C associated with the evolution of 3-pentanone (T_M = 278°C), 2-methyl-1-penten-3-one (T_M = 235°C and shoulder at 280°C), 1-propanol (T_M = 200 and 250°C), 2-methyl-2-pentanal (T_M = 265°C), and a species that has been identified by GC–MS as unsaturated methylcyclopentanone; (iii) a high-temperature peak with maximum at T_M = 408°C originating from desorption of C_1–C_6

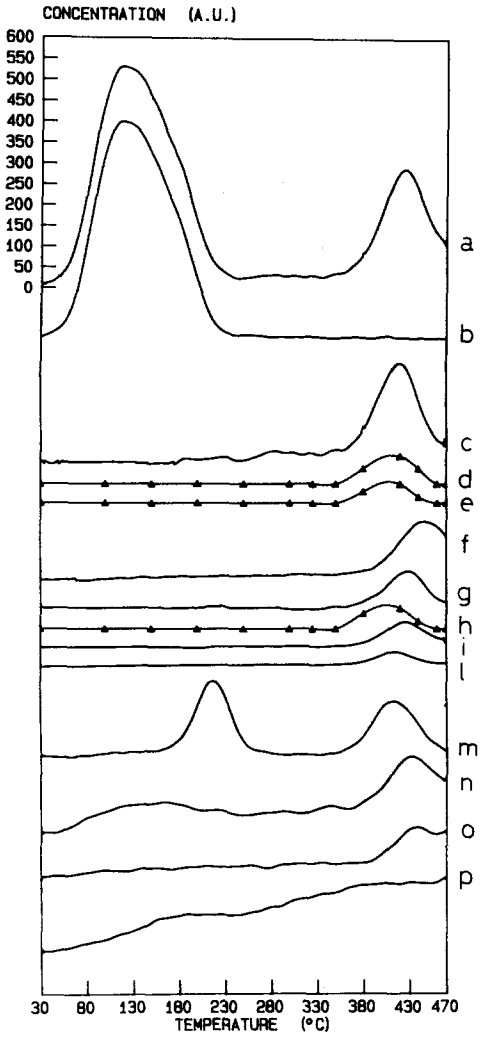

FIG. 1. TPSR traces obtained upon 1-propanol adsorption at 35°C on K-promoted ZnCr oxide. Solid lines, QMD signal; lines with triangles, interpolated experimental points from GC analysis. (a) Overall FID trace; (b) 1-propanol (AMU 31); (c) propylene (AMU 41, ×2); (d) 3-pentanone (×2); (e) 2-butanone (×2); (f) methane (AMU 16, ×2); (g) ethylene (AMU 26, ×2); (h) butenes (×2); (i) benzene (AMU 78, ×2); (l) toluene (AMU 91, ×2); (m) hydrogen (AMU 2); (n) CO (AMU 28); (o) CO_2 (AMU 44); (p) water (AMU 18). Traces (m)–(p) are not scaled with respect to the other desorption profiles.

hydrocarbons (methane, ethylene, propylene, butenes, pentenes, hexadienes), 2-butanone, and aromatics (benzene, toluene, xilenes). In addition, a few more products have been identified, including phenols and methylcyclohexanones.

The QMD desorption profile of methane (T_M = 450°C), hydrogen (T_M = 290 and 405°C), water (T_M = 100°C and shoulder at 200°C, and T_M = 400°C), and carbon dioxide (T_M = 405°C) are shown in Fig. 2B.

n-Propanoic Acid TPSR

The overall FID–TPSR desorption trace and the desorption profiles of the main species obtained upon adsorption of *n*-propanoic acid on K_2O-promoted ZnCrO are shown in Fig. 3. A pronounced high-temperature peak (T_M = 343°C), associated with the evolution of 3-pentanone (T_M = 343°C) and minor amounts of 2-butanone (T_M = 372°C) is apparent in the overall FID–TPSR trace. A broad low-temperature peak (T_M = 100°C), associated with the evolution of *n*-propanoic acid, and a shoulder at T_M = 430°C, which originates from desorption of C_1–C_5 hydrocarbons and aromatics are also evident. Figure 3 also illustrates the desorption peaks of CO_2 (T_M = 334°C), H_2 (T_M = 433°C), CO (T_M = 443°C), and water (a broad peak that extends over the whole *T*-range).

1-Propanol Flow Microreactor Experiments

The results of continuous-flow experiments with 1-propanol as reagent are reported in Table 1. The conversion of 1-propanol is already high at 360°C with C_{2N-1} ketone (3-pentanone), C_N aldehyde (propanal), and C_{2N} aldehyde (2-methylpentanal) as the most abundant products. Minor amounts of C_{N+1} aldehyde (2-methylpropanal), C_{N+1} and C_{2N} primary alcohols (2-methyl-1-propanol and 2-methyl-1-pentanol), C_{2N+1}, C_{2N}, and C_{N+1} ketones (3-heptanone, 2-methyl-3-pentanone, and 2-butanone, respectively), C_{2N-1} secondary alcohol (3-pentanol), and C_1–C_5 hydrocarbons are also observed along with 4-methyl-3-heptanone. In addition to the species listed in Table 1, CO and CO_2 are formed to a significant extent. Trace amounts of other

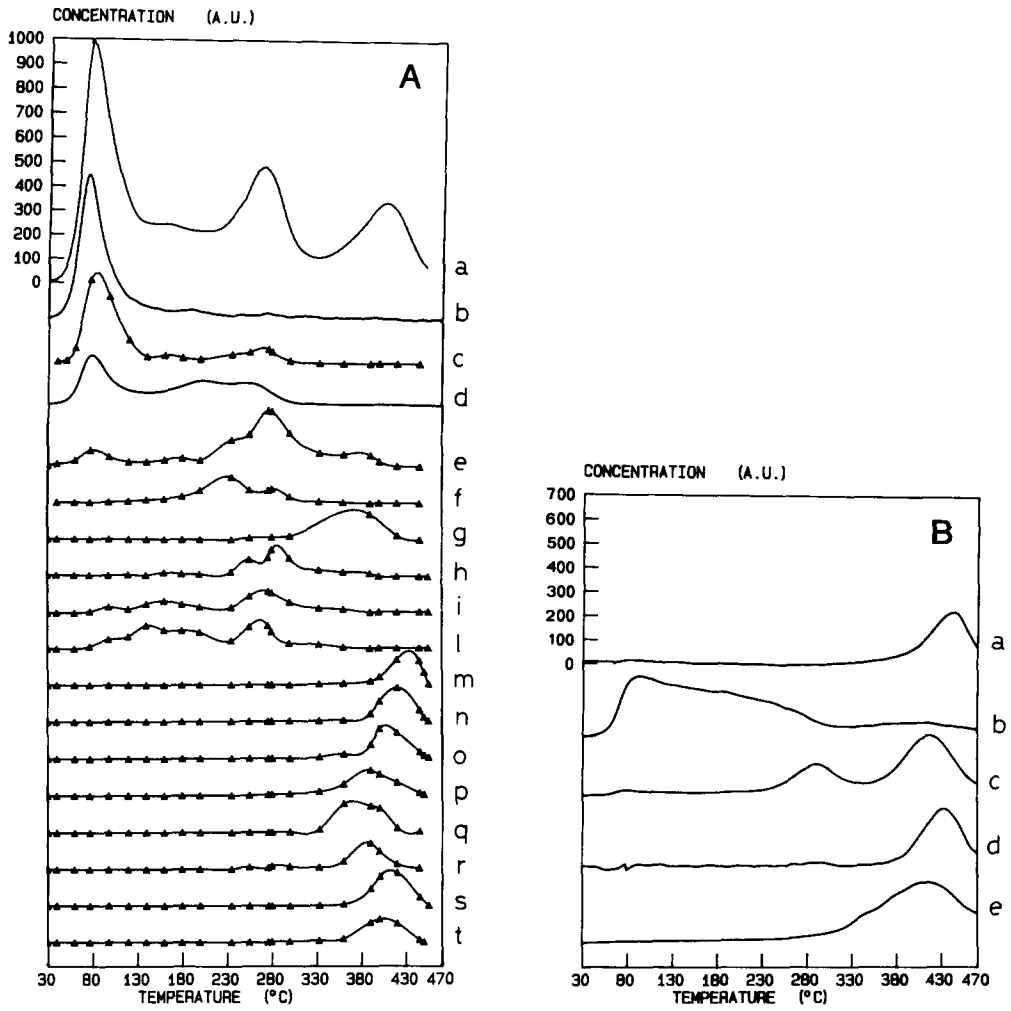

FIG. 2A. TPSR traces obtained upon *n*-propanal adsorption at 35°C on K-promoted ZnCr oxide. Symbols as in Fig. 1(A). (a) Overall FID trace; (b) *n*-propanal (AMU 58); (c) 2-methyl-2-pentenal; (d) 1-propanol (AMU 31, ×8); (e) 3-pentanone (×2); (f) 2-methyl-1-penten-3-one (×2); (g) 2-butanone (×4); (h) phenols (×5); (i) cyclo-hexanone (×2); (l) methyl-cyclo pentanone (×2); (m) ethylene (×5); (n) propylene (×2); (o) butenes (×4); (p) pentenes (×4); (q) hexadienes (×10); (r) benzene (×20); (s) toluene (×4); (t) xilenes (×2). (B) (a) methane (AMU 16, ×8); (b) water (AMU 18); (c) hydrogen (AMU 2); (d) CO (AMU 28); (e) CO_2 (AMU 44). Traces (b)–(e) are not scaled with respect to the other desorption profiles.

oxygenate species were detected by GC–MS analysis of the condensed product, including 2,4-dimethylpentanal, 2-methyl-2-pentenal, 2-hexanone, 3-methyl-2-hexanone, 4-methyl-3-hexanone, 3-methyl-2-butanone, 2,4-dimethyl-3-pentanone, 2-methyl-1-penten-3-one. On increasing the reaction temperature, the conversion of 1-propanol increases and it is almost complete at 405°C. The concentrations of propanal and 2-methylpentanal decrease with temperature, which parallels the changes of the corresponding primary alcohols 1-propanol and 2-methyl-1-pentanol. The concentrations of all the ketones display an opposite behavior and increase with temperature.

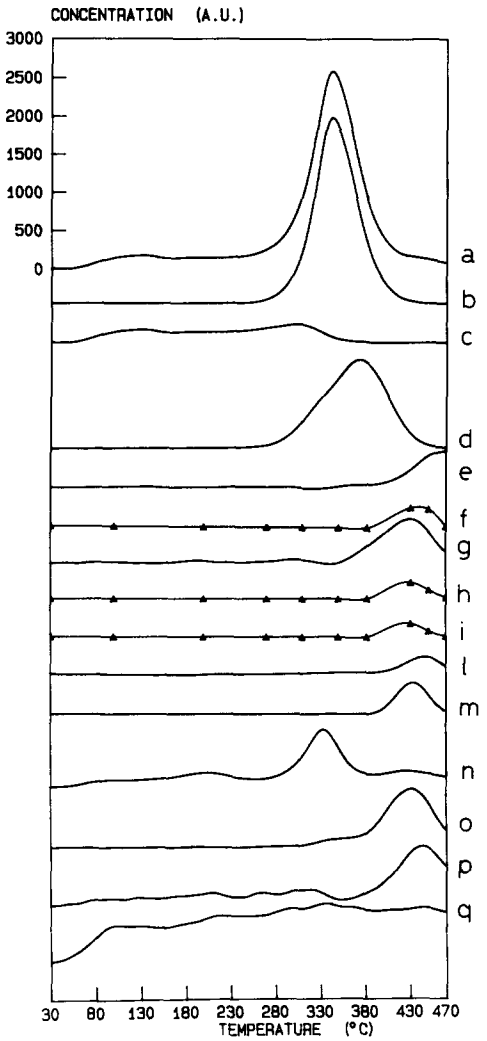

FIG. 3. TPSR traces obtained upon *n*-propanoic acid adsorption at 35°C on K-promoted ZnCr oxide. Symbols as in Fig. 1. (a) Overall FID trace; (b) 3-pentanone (AMU 57); (c) *n*-propanoic acid (AMU 74); (d) 2-butanone (AMU 72, × 10); (e) methane (AMU 16, × 10); (f) ethylene (AMU 26, × 10); (g) propylene (AMU 41, × 10); (h) butenes (× 10); (i) pentenes (× 10); (l) benzene (AMU 78, × 10); (m) toluene (AMU 91, × 10); (n) CO_2 (AMU 44); (o) hydrogen (AMU 2); (p) CO (AMU 28); (q) water (AMU 18). Traces (n)–(q) are not scaled with respect to the other desorption profiles.

The formation of hydrocarbons is favored by raising the temperature.

The results indicate that ketones (particularly 3-pentanone) represent by far the most abundant products formed from 1-propanol over K_2O-promoted ZnCrO at atmospheric pressure. To gain a better insight into the role of ketones as intermediates during 1-propanol flow runs a series of experiments have been performed with 3-pentanone and 2-butanone as reagents.

3-Pentanone Flow Microreactor Experiments

Table 2 reports the results of 3-pentanone continuous-flow experiments. It appears

TABLE 1

Continuous Flow Microreactor Runs of 1-Propanol over K_2O-Promoted ZnCrO

Products	Temperature		
	360°C	385°C	405°C
Alcohols			
1-Propanol	11.0	1.4	0.2
2-Methyl-1-propanol	1.4	0.6	0.7
2-Methyl-1-pentanol	3.1	1.2	0.3
3-Pentanol	0.4	0.4	0.3
	15.9	3.6	1.5
Aldehydes			
Propanal	20.0	4.9	2.0
2-Methyl-propanal	3.9	7.3	5.0
2-Methyl-pentanal	12.6	7.5	2.2
	36.5	19.7	9.2
Ketones			
3-Pentanone	36.9	45.4	40.3
3-Heptanone	2.7	5.1	5.3
4-Methyl-3-heptanone	1.9	3.1	2.7
2-Butanone	1.3	5.4	9.6
2-Methyl-3-pentanone	1.1	5.8	10.1
	43.9	64.8	68.0
Hydrocarbons			
Methane	—	—	0.1
Ethane	—	0.1	0.2
Ethylene	—	0.1	0.2
Propane	—	—	0.2
Propylene	0.5	0.8	1.2
Butenes	—	0.1	1.1
Pentenes	—	0.2	0.9
	0.5	1.3	3.9
Others	3.2	10.6	17.4

Note. Feed: He 19% + H_2 79% + 1-propanol 2%; flow rate = 100 Ncc/min; P = 1 Atm; catalyst weight = 160 mg. Results are given as products weight percentage on a (CO_x + H_2O) free basis.

TABLE 2

Continuous Flow Microreactor Runs of 3-Pentanone over K-Promoted ZnCrO

Products	Temperature		
	360°C	385°C	405°C
3-Pentanone	88.0	78.8	76.7
2-Butanone	1.4	3.1	4.0
3-Methyl-2-butanone	0.3	0.9	1.2
2-Methyl-3-pentanone	2.9	7.5	8.5
3-Pentanol	1.3	0.8	0.7
C_1–C_3 hydrocarbons	0.8	1.4	2.3
Butenes	0.5	1.7	2.0
Pentenes	4.6	5.6	4.8
Others	0.7	0.7	0.5

Note. Feed: He 19% + H_2 79% + 3-pentanone 2%; flow rate = 100 Ncc/min; P = 1 Atm; catalyst weight = 160 mg. Results are given as weight percentage on a (CO_x + H_2O) free basis.

that the reactivity of 3-pentanone is much lower than that of 1-propanol. The main reaction products are pentenes, 3-pentanol, and other oxygenates and hydrocarbons (namely 2-butanone, 2-methylbutanone, 2-methyl-3-pentanone, C_1–C_3 hydrocarbons and butenes). On increasing the reaction temperature, the formation of 2-butanone, 2-methyl-3-pentanone, and hydrocarbons is favored, whereas 3-pentanol is produced to a lower extent. Accordingly the mole ratio 3-pentanone/3-pentanol significantly increases with temperature (3-pentanone/3-pentanol = 68 at 360°C, 98 at 385°C, and 110 at 405°C).

2-Butanone Flow Microreactor Experiments

Table 3 shows the results of 2-butanone continuous-flow experiments. Butenes are the most abundant products; minor amounts of 2-butanol, 3-pentanone, 3-heptanone, and 5-methyl-3-heptanone are also detected. The conversion of 2-butanone decreases with temperature; similar trends are observed in the formation of 2-butanol and of butenes. The amounts of 3-heptanone and 5-methyl-3-heptanone also decrease with temperature, whereas 3-pentanone and pentenes are slightly enhanced.

DISCUSSION

Reactivity of K_2O-Promoted ZnCr Oxide

A comparison between the TPSR spectra presented in this work with those obtained upon adsorption of linear C_4 oxygenates over the same catalyst and reported in a previous paper (*27*) indicates that similar catalyst functions are involved in the reaction/decomposition pathways of C_3 and C_4 alcohols, aldehydes and acids over K-promoted ZnCr oxide. Indeed it appears that: (i) C_N alcohols, C_N and C_{N-1} olefins, and C_{2N-1} ketones are the primary species obtained upon adsorption of 1-propanol and 1-butanol; (ii) C_N alcohols, C_N and C_{2N} aldehydes, C_N and C_{N-1} olefins, and C_{2N}, C_{2N-1}, and C_{N+1} ketones are desorbed in the case of *n*-propanal and *n*-butanal; and (iii) C_N acids, C_{N-1} olefins, and C_{2N-1} and C_{N+1} ketones are formed in the case of *n*-propanoic and *n*-butanoic acid.

The desorption of the different products during TPSR of linear C_4 oxygenates over

TABLE 3

Continuous Flow Microreactor Experiments of 2-Butanone over K-Promoted ZnCrO

Products	Temperature		
	360°C	385°C	405°C
2-Butanone	67.5	72.3	73.4
2-Methyl-butanone	0.2	1.1	2.1
3-Pentanone	1.1	1.4	1.9
2-Methyl-3-pentanone	0.1	0.3	0.3
3-Heptanone	1.2	0.6	0.4
5-Methyl-3-heptanone	0.8	0.4	0.2
6-Methyl-3-heptanone	—	0.1	0.1
2-Butanol	1.9	1.4	1.1
C_1–C_3 hydrocarbons	0.8	1.4	2.3
Butenes	23.1	18.4	15.6
Pentenes	1.5	1.5	1.5
Other	1.8	1.1	1.0

Note. Feed: He 19% + H_2 79% + 2-butanone 2%; flow rate = 100 Ncc/min; P = 1 Atm; catalyst weight = 160 mg. Results are given as weight percentage on a CO_x + H_2O free basis.

the same catalyst has been previously explained by invoking the desorption/decomposition of C_N–C_{2N} intermediate surface species (*27*) whose presence, on the catalyst surface, has been confirmed by DRIFT–FTIR experiments (*28*). These species include C_4 and C_8 alkoxide, carboxylate, and molecularly adsorbed aldehyde molecules. The corresponding C_3 and C_6 species are likely involved during TPSR of C_3 oxygenates. Accordingly (i) a surface C_6 aldol intermediate is involved in aldolic-type condensation of two *n*-propanal molecules and accounts for the formation of C_{2N} aldehyde (2-methyl-2-pentanal) and C_{2N} ketone (2-methyl-3-pentanone); (ii) dehydration or hydrolysis of a C_3 alkoxide intermediate originates the C_N olefin (propylene) or the C_N alcohol (1-propanol), respectively; (iii) decarboxylation of a C_3 carboxylate species leads to ethylene desorption; and (iv) decarboxylation of a C_6 carboxylate intermediate is responsible for the desorption of the C_{2N-1} ketone (3-pentanone). The origin of the C_{N+1} ketone (2-butanone) in *n*-propanal and *n*-propanoic acid TPSR is not yet completely understood: this point will be addressed in the following sections.

Additional minor species have been identified among desorbed products, including methane, aromatics, and ketones. They are likely formed either by decomposition of heavy surface intermediates or by consecutive reactions of the primary desorbed products. Thus the formation of methane at high temperature may be explained by cracking, whereas aromatics (benzene and toluene) are possibly produced by aromatization of light olefins.

The results of flow microreactor experiments of 1-propanol, 3-pentanone, and 2-butanone compare well with TPSR data of C_3 and C_4 oxygenate molecules as far as the nature of the reaction products are considered, indicating that the same chemical reactions and associated catalyst functions account for both transient (TPSR) and steady-state (flow microreactor runs) conditions. Thus it appears that the following chemical routes, as schematically represented in Fig. 4, are effectively catalyzed by a K_2O-promoted ZnCrO catalyst.

(a) Alcohol dehydrogenation (step I in Fig. 4):

$$\text{primary alcohol} \rightarrow \text{aldehyde} + H_2$$

(e.g., 1-propanol $\rightarrow$ *n*-propanal)

(b) Normal aldolic-type condensation (step II + N in Fig. 4):

$$2C_N \text{ aldehyde} \rightarrow C_{2N} \text{ aldehyde} + H_2O$$

(e.g., 2-*n*-propanal $\rightarrow$ 2-methylpentanal)

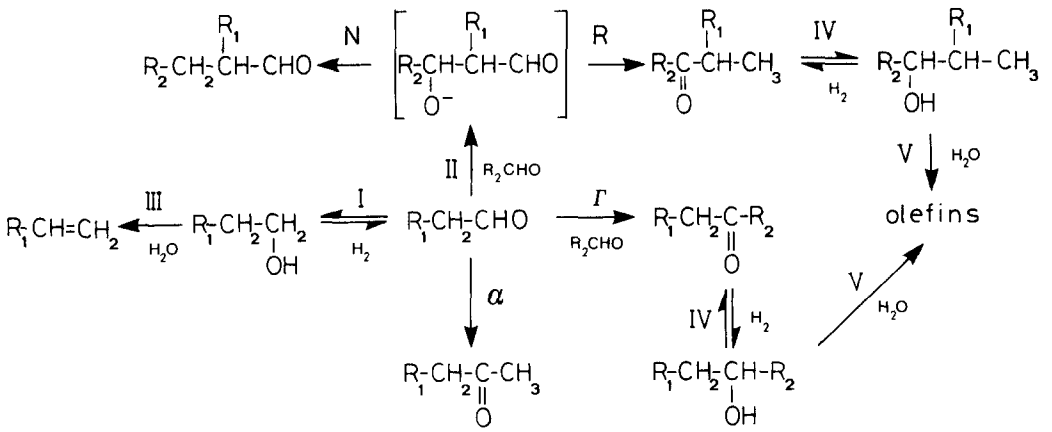

FIG. 4. Reaction pattern for HAS over K-promoted ZnCr oxide.

(c) Reversal aldolic-type condensation (step II + R in Fig. 4):

$$2C_N \text{ aldehyde} \rightarrow C_{2N} \text{ ketone} + H_2O$$

(e.g., 2-*n*-propanal → 2-methyl-3-pentanone)

(d) Aldehyde or ketone hydrogenation (step I and IV in Fig. 4):

$$\text{aldehyde} + H_2 \rightarrow \text{primary alcohol}$$

(e.g., 2-methylpentanal → 2-methyl-1-pentanol)

$$\text{ketone} + H_2 \rightarrow \text{secondary alcohol}$$

(e.g., 3-pentanone → 3-pentanol)

(e) Ketonization (step Γ in Fig. 4):

$$2C_N \text{ aldehyde} + O_{(l)} \rightarrow C_{2N-1} \text{ ketone} + CO_2 + H_2$$

or

$$2C_N \text{ acid} \rightarrow C_{2N-1}\text{ketone} + CO_2 + H_2O + O_{(l)}$$

where (l) represents a lattice oxygen atom

(e.g., 2-*n*-propanal or 2-*n*-propanoic acid → 3-pentanone)

(f) Reversal α-addition (step α in Fig. 4):

$$C_N \text{ aldehyde} + C_1 \rightarrow C_{N+1} \text{ ketone}$$

(e.g., *n*-propanal → 2-butanone)

(g) Alcohol dehydration (steps III and V in Fig. 4):

$$C_N \text{ alcohol} \rightarrow C_N \text{ olefin}$$

(e.g., 1-propanol → propylene)

(h) Decarboxylation

$$C_N \text{ acid} \rightarrow C_{N-1} \text{ olefin} + CO_2$$

(e.g., *n*-propanoic acid → ethylene + CO_2)

Reactions (a)–(h) are discussed in detail in the following.

Hydrogenation/Dehydrogenation of Carbonylic Molecules

The presence of aldehyde/primary alcohol and ketone/secondary alcohol pairs among the products of flow experiments indicates that the dehydrogenation of alcohols to the corresponding aldehydes as well as the hydrogenation of carbonyl compounds to the corresponding alcohols are effectively catalyzed under the experimental conditions of the present study. Indeed all the C_N primary alcohols originated from C_N aldehydes detected in 1-propanol flow microreactor runs have been observed among the reaction products, including 1-propanol/propanal, 2-methyl-1-propanol/2-methylpropanal, and 2-methyl-1-pentanol/2-methylpentanal (see Table 1). On the other hand, secondary alcohols have been detected only when ketones are present in significant amounts: accordingly 3-pentanol has been observed only during 1-propanol and 3-pentanone flow experiments (where 3-pentanone is present in large amounts; Tables 1 and 2), whereas 2-butanol has been detected only during 2-butanone flow experiments (Table 3). Figures 5 and 6 compare the partial pressure ratio K_p of the aldehyde and ketone hydrogenation reactions, respectively, evaluated from the experimental concentrations of reactants and products, with the corresponding equilibrium constant K_{eq}, estimated from thermodynamic relationships, for the aldehyde/primary alcohol and ketone/secondary alcohol pairs identified among the reaction products. Equilibrium is clearly established at the conditions of the present study for both aldehyde and ketone hydrogenations:

$$C_N \text{ aldehyde} + H_2 \Leftrightarrow C_N \text{ primary alcohol}$$

$$C_N \text{ ketone} + H_2 \Leftrightarrow C_N \text{ secondary alcohol}$$

Deviations from thermodynamic predictions are apparent at temperatures below 405°C: they are of positive sign in the case of *n*-propanal hydrogenation and of negative sign in the other cases, indicating that 1-propanol is dehydrogenated to the corre-

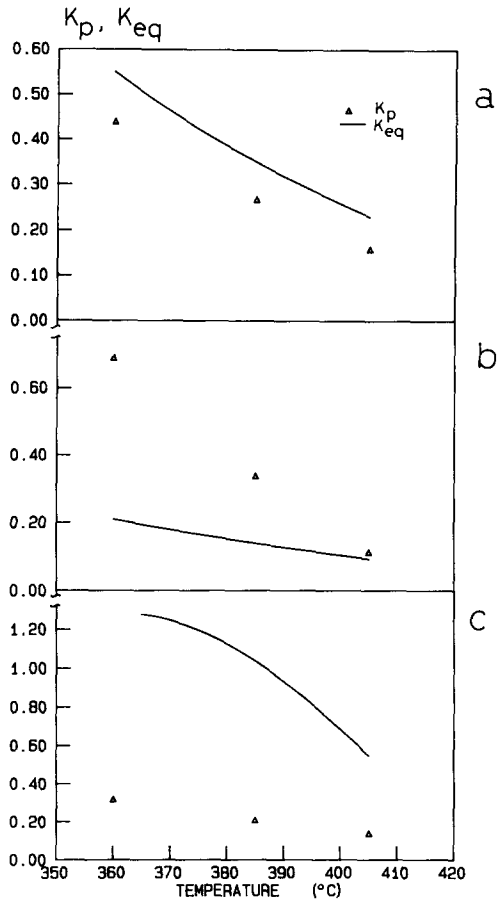

FIG. 5. Comparison between partial pressure ratio K_p and equilibrium constant K_{eq} for aldehydes/primary alcohols equilibria: (a) 2-methyl-propanal + $H_2 \rightarrow$ 2-methyl-1-propanol. (b) *n*-propanal + $H_2 \rightarrow$ 1-propanol. (c) 2-methyl-pentanal + $H_2 \rightarrow$ 2-methyl-1-pentanol.

sponding aldehyde, whereas other alcohols are produced by hydrogenation of the corresponding aldehydes or ketones. It is worth noting that the low concentration of secondary alcohols in the liquid product is dictated by the values of the equilibrium constants of ketone hydrogenations, which are one order of magnitude lower than those of aldehyde hydrogenations.

The hydrogenating/dehydrogenating capability of K_2O-promoted ZnCrO is also apparent during TPSR experiments: 1-propanol is formed in *n*-propanal TPSR already at low temperature, whereas at high temperatures the desorption of aromatics and hydrogen in 1-propanol, *n*-propanal, and *n*-propanoic acid TPSR is indicative of the occurrence of dehydrogenation reactions. Furthermore, a dehydrogenation step is likely involved in the formation of carboxylate species from the corresponding alkoxide and aldehyde molecules, as discussed below.

The hydrogenation/dehydrogenation functions revealed by this study were also apparent in TPSR and flow experiments of C_4 oxygenates over the same catalyst (*24–28*) and are quite effective under HAS conditions: this is indicated, e.g., by the close approach to chemical equilibrium between aldehydes and primary alcohols and between ketones and secondary alcohols (*29, 30*) and by the fact that similar changes in product distribution are observed upon addition of, e.g., ethanol or acetaldehyde to the (CO + H_2) mixture (*30*).

It is noteworthy that the strong hydrogenating/dehydrogenating reactivity of the

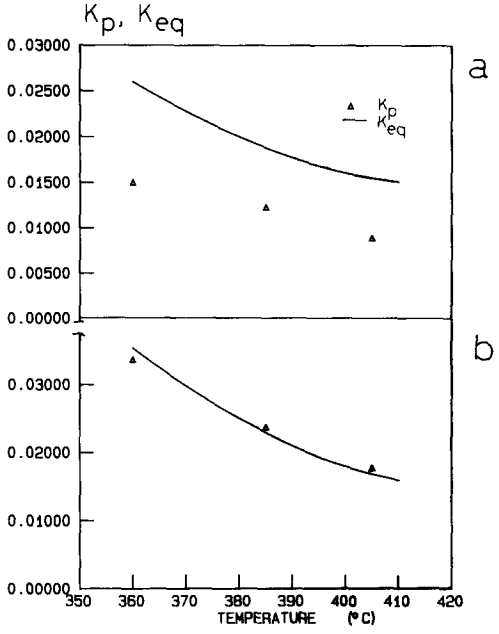

FIG. 6. Comparison between the partial pressure ratio K_p and equilibrium constant K_{eq} for ketones/secondary alcohols equilibria: (a) 3-pentanone + $H_2 \rightarrow$ 3-pentanol. (b) 2-butanone + $H_2 \rightarrow$ 2-butanol.

ZnCrO catalyst is not apparent in the hydrogenation of the olefins to the corresponding paraffins. Indeed the experimental partial pressure ratios of the hydrogenation reactions of ethylene and propylene are lower by orders of magnitude than the corresponding equilibrium constants.

Aldolic-type Condensations

(a) *"Normal" Aldolic-type Condensation*

The formation of large amounts of 2-methyl-2-pentenal and water in *n*-propanal TPSR is supportive of aldolic-type condensation of *n*-propanal followed by dehydration of the aldol intermediate (A):

$$2CH_3CH_2CHO \rightarrow \underset{\text{(A)}}{CH_3CH_2\underset{\displaystyle OH}{\underset{|}{C}}\underset{\displaystyle CH_3}{\underset{|}{C}}HCHO} \rightarrow CH_3CH_2CH{=}\underset{\displaystyle CH_3}{\underset{|}{C}}CHO + H_2O$$

The same catalytic function is likely involved in the formation of 2-methylpentanal in flow experiments of 1-propanol. In this case, the presence of hydrogen at high temperature favors the hydrogenation of the internal C=C bond of 2-methyl-2-pentenal to give 2-methylpentanal: this is proved by flow experiments performed with 1-propanol in pure He where large amounts of 2-methyl-2-pentenal and other unsaturated compounds were formed.

Aldolic-type condensations are believed to generate quite a few other reaction products among those detected in 1-propanol flow experiments. Thus condensation of a C_1 oxygenate intermediate (possibly a species related to formaldehyde) with *n*-propanal is invoked to explain the presence of remarkable amounts of 2-methylpropanal:

$$HCHO + CH_3CH_2CHO + H_2 \rightarrow \underset{\displaystyle CH_3}{\underset{|}{C}}HCHO + H_2O$$

The nature and the origin of the C_1 intermediate have not yet been completely understood. In a series of flow experiments performed with 1-propanol + methanol feed mixture (1-propanol/methanol $\approx$ 1 by volume) a significant increase of 2-methylpropanal was observed, suggesting that methanol is first dehydrogenated to a C_1 reactive species (possibly formaldehyde), which then participates in the chain growth via condensation reactions. Concerning the origin of the C_1 intermediate, it is worth mentioning that evidence has been collected for the occurrence of ketonization reactions leading to ketones and CO_2 on unpromoted and K_2O-promoted ZnCrO catalysts (see Section 3) (*24–28*). It has been proposed that CO_2 originates from a surface formate (*17*), which could be likely hydrogenated by surface hydrides to formaldehyde or methanol. Indeed recent TPD and flow microreactor experiments of formic acid over the same K_2O-promoted ZnCrO catalyst confirmed that surface formate species are hydrogenated to formaldehyde and methanol at $T >$ 200°C (*31*). Thus in the following we refer to formaldehyde as a possible C_1 intermediate species participating in aldolic-type condensations. The possibility that CO (which is detected among reaction products) might be involved in the formation of formaldehyde or methanol at atmospheric pressure has been ruled out since no significant changes in the product distribution have been observed by replacing the H_2 + 20% He carrier gas with CO + H_2 (CO/H_2 = 1).

In addition to 2-methylpentanal and 2-methylpropanal, other species can be formed via aldolic-type condensations during *n*-propanal TPSR and 1-propanol, 3-pentanone, and 2-butanone flow microreactor runs, as schematically depicted in Table 4. All of the aldehydes and ketones detected among the reaction products may be involved in aldolic-type condensations. However, different reactivities are expected for the various carbonyl species on the basis of their molecular structure. The carbonyl species are considered as electrophilic or nucleophilic reactants.

TABLE 4

Schematic Representation of Electrophilic and Nucleophilic Species Involved in Aldolic-type Condensation Reactions and Products Originating Therefrom According to the "Normal" and "Reversal" Modes

Electrophilic molecules	Nucleophilic molecules	Products originating from aldolic-type condensations	
		Normal mode	Reversal mode
CCC(=O)	C$\bar{C}$C(=O)	C(CCCC(=O))C (a)	C(CCCC(=O))C (l)
CCC(=O)	CCC$\bar{C}$(=O)	CCCCCCC(=O) (b)	CCCCCCC(=O) (m)
CCC(=O)	C$\bar{C}$CC(=O)	C(CCCC(=O))C (c)	C(CCCC(=O))C (n)
CCC(=O)	C$\bar{C}$CCC(=O)	C(CCCCCC(=O))C (d)	C(CCCCCC(=O))C (o)
C(=O)	C$\bar{C}$C(=O)	C(CC(=O))C (e)	C(CC(=O))C (p)
C(=O)	CCC$\bar{C}$(=O)	CCCCC(=O) (f)	CCCCC(=O) (q)
C(=O)	C$\bar{C}$CC(=O)	C(CCC(=O))C (g)	C(CCC(=O))C (r)
C(=O)	C$\bar{C}$CCC(=O)	C(CCCC(=O))C (h)	C(CCCC(=O))C (s)
C(CC(=O))C	C$\bar{C}$C(=O)	C(C)(CCCC(=O))C (i)	C(C)(CCCC(=O))C (t)

(a1) *Electrophilic reactants.* In Table 4 only aldehydes are regarded as electrophilic reagents. Indeed all the expected products of aldolic-type condensations involving aldehydes as electrophilic reactants have been detected in 1-propanol flow experiments (Table 4, species a–i). On the contrary only minor quantities of 5-methyl-3-heptanone (Table 3), the expected product of self-condensation of 2-butanone, have been detected during 2-butanone flow experiments and no aldolic-type condensation product of 3-pentanone (Table 2) has been observed during 3-pentanone flow experiments.

The relative amounts of species a–i (Table 4) observed in 1-propanol flow experiments call for a different reactivity of linear and branched aldehydes as electrophilic reactants. In fact minor amounts of 2,4-dimethylpentanal (species i) are formed from 2-methylpropanal as electrophilic agent and no products have been detected originating from 2-methylpentanal again as electrophilic species, in spite of the reasonably high concentrations of these reagents. This indicates a much lower reactivity of 2-methyl-branched aldehydes as compared to linear aldehydes. It is believed that the methyl substituent in the α position with respect to the carbonyl group decreases the electrophilic character of the molecule, due to steric and electronic factors.

(a2) *Nucleophilic reactants.* Linear C_{2+} aldehydes (*n*-propanal) and linear ketones are listed in Table 4 as nucleophilic reactants. Condensations involving α-branched nucleophilic agents have been ruled out on the basis of the observed product distribution and in line with previous results of 2-methylpropanal TPSR (*27*) and of chemical enrichment experiments with *i*-butanol added to the CO + H_2 mixture (*32*). In both cases no evidence was collected in favor of cross aldol-type condensation of 2-methylpropanal. The presence of branching in the α-position with respect to the carbonyl group is expected to prevent the formation of the carbanion.

The results of 1-propanol, 3-pentanone, and 2-butanone flow experiments indicate that ketones participate as nucleophilic species in aldolic-type condensation reactions, which eventually accounts for the formation of 3-heptanone (species b) and 3-methyl-2-

hexanone (species c, 2-butanone + *n*-propanal), 4-methyl-3-heptanone (species d, 3-pentanone + *n*-propanal), 3-pentanone (species f) and 3-methyl-2-butanone (species g, 2-butanone + formaldehyde), and 2-methyl-3-pentanone (species h, 3-pentanone + formaldehyde).

It is noteworthy that any asymmetric ketone (e.g., 2-butanone) may originate, upon hydrogen abstraction, two distinct nucleophilic species: indeed aldolic-type condensation of 2-butanone with *n*-propanal results in the formation of 3-heptanone (species b) and of 3-methyl-2-hexanone (species c). The greater amounts of 3-heptanone as compared to 3-methyl-2-hexanone observed during 1-propanol flow experiments indicate that hydrogen abstraction occurs preferentially on the $-CH_3$ group rather than on the $-CH_2-$ group. The same argument applies in explaining the small amounts of 4-methyl-3-heptanone (species d, the expected product of condensation of *n*-propanal with 3-pentanone) obtained in 1-propanol flow experiments. Indeed the reactivity of the methyl group of 2-butanone in the formation of the carbanion is higher than that of the methylene group in 3-pentanone and this eventually accounts for similar concentrations of 3-heptanone and 4-methyl-3-heptanone in Table 1 in spite of the much greater concentration of 3-pentanone.

(*b*) *"Reversal" Aldolic-type Condensation*

It has recently been proved by experiments with labeled molecules that aldolic-type condensation reactions over Cs-promoted low-*T* methanol catalyst can occur in a particular fashion, quoted as "oxygen retention reversal" or simply "reversal" (*5, 12, 15, 17, 33*). The mechanism of the reversal mode (Path II + R in Fig. 4) is based on the retention of the anionic oxygen of the aldol intermediate (A) and on the hydrogenation of the carbonyl group, and eventually accounts for the formation of ketones:

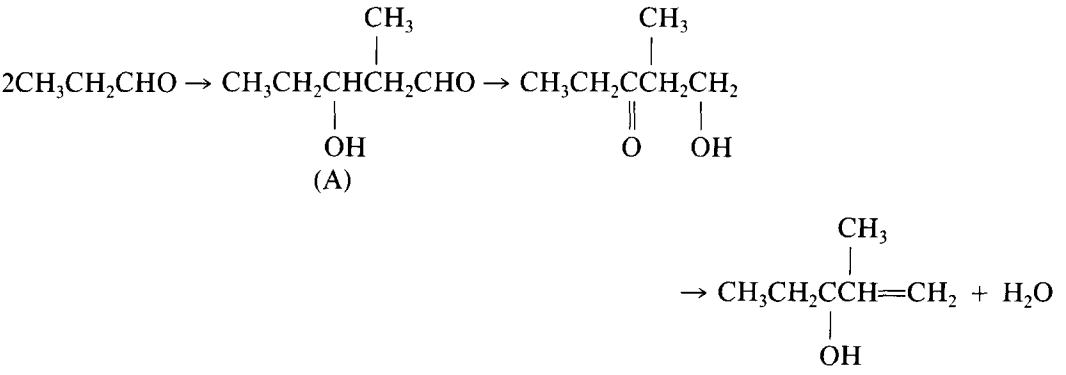

The desorption of significant amounts of 2-methyl-1-penten-3-one (the expected product of the reversal aldolic condensation of *n*-propanal) at 160–320°C with the evolution of 2-methyl-2-pentenal (which originates from normal aldolic-type condensation) during *n*-propanal TPSR clearly shows that both reversal and normal aldolic-type condensations operate over K_2O-promoted ZnCrO catalyst. The occurrence of two desorption peaks of 2-methyl-2-pentenal further suggests that different active sites are present on the catalyst surface: one, responsible for "normal" aldolic-type condensation, is active already at low temperature, whereas the other site possibly stabilizes the aldol intermediate and promotes the reverse mode. Since it has been proposed that aldolic-type condensation with oxygen retention reversal is specific of alkali promoters [5, 12], the second site could likely be associated with K_2O.

The occurrence of reverse aldolic-type condensation reactions over K_2O-promoted ZnCrO is further supported by the results of 1-propanol flow experiments considering that significant amounts of 2-methyl-3-pentanone have been detected (Table 1). 2-Methyl-3-pentanone can be formed by hydrogenation of 2-methyl-1-penten-3-one which in turn originates from the reverse condensation of two molecules of *n*-propanol. Note that although 2-methyl-3-pentanone is also the expected product of ketonization reaction involving 2-methyl-propanal and n-propanal (see next section), this cannot apply to TPSR measurements (where 2-methyl-1-penten-3-one was observed) since 2-methyl-propanal was not detected in this case.

The presence of other ketones in flow experiments can be explained by the occurrence of aldolic-type condensations with oxygen retention reversal too. Table 4 shows, for all the species involved in normal aldolic-type condensations, the expected reverse products. It is worth noting that almost all of the reverse products have been identified among the reaction products; species that have been detected in trace amounts or have not even been detected (e.g., 4-methyl-3-hexanone and *n*-pentanal, species n and q, respectively) originate from poorly reactive agents.

As previously illustrated for 2-methyl-3-pentanone, other routes may be responsible for the formation of the products of reverse aldol-type condensations, including ketonization reactions. In a few cases the other route may be the normal aldolic-type condensation reaction, since both normal and reversal modes lead to the same species (e.g., 3-heptanone, species b in Table 4).

Ketonization Reactions

In line with previous suggestions provided to explain the desorption of C_{2N-1} ketones + CO_2 during TPSR of C_4 linear and branched oxygenates (*24–28*), the desorption of 3-pentanone during TPSR of 1-propanol, *n*-propanal, and *n*-propanoic acid can be associated with the decomposition of a surface C_6 hydroxy carboxylate intermediate (B):

$$\underset{\text{(B)}}{\mathrm{CH_3CH_2\overset{\mathrm{OH}}{\overset{|}{C}}HCH(CH_3)COO_{(a)}}} \rightarrow \mathrm{CH_3CH_2\overset{\mathrm{O}}{\overset{\|}{C}}CH_2CH_3} + CO_{2(a)} + H_{(a)}$$

where (a) represents an adsorbed surface species. According to the above scheme, equimolar desorption of 3-pentanone and CO_2 is expected. In our experiments, calibration of the mass spectrometer was not attempted, which prevented comparison of the amounts of CO_2 and 3-pentanone desorbed.

The formation of the surface intermediate (B) may involve surface oxidation by lattice oxygen of the aldol intermediate (A) or, alternatively, condensation of a molecularly adsorbed aldehyde with a surface carboxylate species or condensation of two carboxylate species (*27*). In the case of 1-propanol TPSR the carboxylate species is likely formed by oxidation of surface alkoxide species. Spectroscopic evidence has been provided for the presence and reactivity of such carboxylate species (*25, 28*). As in the case of C_4 linear oxygenates the desorption of the C_{2N-1} ketone occurs at different temperatures in TPSR runs with 1-propanol (420°C), *n*-propanal (78 and 278°C), and *n*-propanoic acid (343°C) since different surface intermediate species are believed to participate in the desorption process (*25, 27*). It should be noted that formation of the C_{2N-1} ketone occurs in the low-T region in the case of *n*-propanal TPSR, as observed also for *n*-butanal (*25, 27*). In this case 3-pentanone may originate from aldolic-type condensation followed by decarbonylation of the aldol intermediate. CO was actually not detected; however, this may be due to its

TABLE 5

Aldehydic Molecules Involved in Ketonization Reactions and Products Originating Therefrom

Aldehydic molecules		Product
CCC‖O	CCC‖O	CCCCC‖O
C CCC‖O	CCC‖O	C CCCCC‖O
C CCC‖O	C CCC‖O	C C CCCCC‖O
C CCCCC‖O	CCC‖O	C CCCCCCC‖O
C CCCCC‖O	C CCC‖O	C C CCCCCC‖O

concentration being below the detection threshold of the mass spectrometer.

The formation of 3-pentanone in flow experiments is believed to occur with similar mechanisms (route Γ in Fig. 4). 3-Pentanone is the most abundant reaction product in the investigated temperature range: this indicates that ketonization is one of the major catalytic functions of K_2O-promoted ZnCrO under the conditions of the present study. As a matter of fact, all the expected ketones originating from ketonization of the detected aldehydes have been observed, as summarized in Table 5. Comparison of Table 5 with Table 4 suggests that ketonization represents an alternative route for the synthesis of ketones with respect to reverse aldolic-type condensation reaction.

Thermodynamic analysis shows that the formation of ketones by ketonization under HAS conditions is limited by the inverse cubic dependence of the partial pressure ratio on the total pressure according to the stoichiometry:

$$R_1CH_2OH + R_2CH_2OH \Leftrightarrow R_1CR_2{=}O + CO + 3H_2$$

The departures from thermodynamic equilibrium at low temperatures and short contact times further indicate that ketones are consumed via ketonizations and that they are formed via reverse aldolic-type condensations (*30*). This eventually provides additional evidence in favor of the relevance of aldolic-type condensations with oxygen retention reversal over high-*T*-modified methanol catalysts.

Ketonizations of carboxylic surface intermediates and aldolic-type condensation reactions with oxygen retention reversal involving aldehydic molecules have also been invoked by Elliott and Pennella to explain the formation of C_{2N} and C_{2N-1} ketones in a series of experiments performed with linear primary alcohols (ethanol, 1-propanol, 1-butanol) at 285°C and 1 to 65 Atm over CuO/ZnO/Al_2O_3 catalyst (*17*).

Reversal α-Addition

α-Addition with oxygen retention reversal (ORR) mechanism (identified in the following as reversal α-addition) is proposed to account for the formation of 2-butanone during 1-propanol flow microreactor runs. Reversal α-addition is regarded as a reaction between a C_1 oxygenate species (indicated as CO) and a C_N aldehyde to originate the C_{N+1} 2-ketone (route α in Fig. 4):

$$CH_3CH_2CHO + CO + H_2 \rightarrow CH_3CH_2C{=}OCH_3$$

Evidence has been provided for the existence of a linear chain growth step via C_1 addition in the synthesis of higher oxygenates over a Cs-promoted Cu/ZnO catalyst (*12, 5*). The proposed mechanism involves the nucleophilic attack at the α-carbon of an

adsorbed aldehydic intermediate by a formyl species to originate a linear C_{N+1} aldehyde.

In our case, formation of the C_{N+1} 2-ketone during 1-propanol flow-microreactor experiments may involve a related mechanism; however, in this case the C_{N+1} dioxygenate species (C) apparently loses the oxygen of the formyl species rather than that of the aldehydic compound:

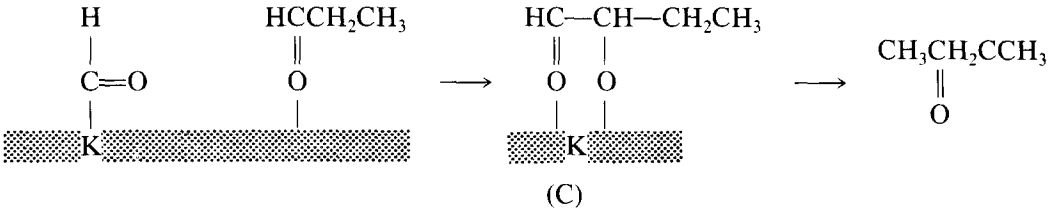

(C)

Since the retention of the aldehydic oxygen recalls the mechanism of aldolic-type condensations with oxygen retention reversal, α-addition has been regarded as a reversal reaction. As for aldolic-type condensation, the alkali promoter may play a role in the proposed mechanism by stabilizing the oxygen of the carbonyl species and thus originating the ketone molecule rather than the aldehyde. The formation of the C_{N+1} ketone (2-pentanone) has also been observed during *n*-butanal TPSR (*27*) and flow-microreactor experiments (*31*) over the same K-doped catalyst.

The formation of C_{N+1} ketones by reversal α-addition apparently contrasts with results over Cu-based catalysts reported by Klier and co-workers (*5*) and by Elliott and Pennella (*17*). However, such differences may be rationalized in view of the unequal conditions adopted in the various experiments. Reversal α-addition is favored: (i) by high temperatures (the concentration of 2-butanone in 1-propanol flow experiments is higher at 405°C); (ii) by the presence of the alkali promoter (the products of reversal α-addition were not detected over an unpromoted ZnCrO catalyst (*35*)); and (iii) by a low pressure (thermodynamics limit ketone concentrations in the product mixture under HAS conditions due to the reverse of ketonization reactions (*30*)). All of these favorable conditions were met in our experiments. On the other hand, Elliott and Pennella (*17*) performed 1-propanol flow-microreactor experiments at low temperature (285°C) over an unpromoted $CuO/ZnO/Al_2O_3$ catalyst, whereas Klier and co-workers (*5*) operated with a Cs-promoted catalyst but at low temperatures (250–300°C) and high pressure (7.6 MPa). Thus, in both cases the occurrence of reversal α-addition is expected to be of minor importance, which eventually accounts for the different results obtained over ZnCrO catalyst.

The nature and the origin of the C_1 oxygenate intermediate, which participates as nucleophilic reagent in the reaction, has not been completely clarified yet. Methanol addition to 1-propanol feed, as previously mentioned (see aldolic-type condensations), does not result in a significant increase of 2-butanone. This eventually rules out the direct participation of methanol or formaldehyde in this reaction. However, as previously discussed, the C_1 reactive intermediate may originate from an oxygenate C_1 species that is formed during ketonization reactions. As a matter of fact, 2-butanone evolution in both *n*-propanal and *n*-propanoic acid TPSR runs parallels CO_2 desorption (see Figs. 2A, 2B, and 3). This indicates that the nucleophilic character of the C_1 intermediate is more likely associated with surface species produced from decarboxylation reactions (which originate "native"

CO_2) than with species produced from methanol, as suggested also by the results of the runs with methanol addition to the feed. The same C_1 nucleophilic surface species is possibly involved in the formation of the first carbon–carbon bond in the chain growth mechanism: aspects related to the $C_1 \rightarrow C_2$ step are presently under investigation in our labs (*31*).

The expected products of reversal α-addition on 2-methyl branched aldehydes, namely 3-methyl-2-butanone (from 2-methylpropanal) and 3-methyl-2-hexanone (from 2-methylpentanal), have been observed in amounts smaller than 2-butanone. This may be explained by invoking an inhibiting effect of β-branching on reversal α-addition. Similar conclusions have been reached by Nunan *et al.* (*5*), which attributed the absence of significant amounts of those products that would result from linear C_1 growth over β-branched aldehydes to electronic and steric restrictions. Small amounts of 2-butanone were also observed in 3-pentanone flow experiments. This raises the question whether 2-butanone might be originated from 3-pentanone during 1-propanol flow-microreactor runs. Indeed the ratio 3-pentanone/2-butanone in 3-pentanone flow experiments is much higher than that in 1-propanol flow experiments: accordingly an alternative route that accounts for the formation of 2-butanone should operate, and this is believed to be reversal α-addition over *n*-propanal.

Dehydration

The results of 1-propanol flow-microreactor experiments indicated that 1-propanol is dehydrated to propylene, whereas butenes and pentenes are apparently formed at the expense of C_4 and C_5 oxygenates (e.g., 2-butanone, 2-methyl-1-propanol, and 3-pentanone). Also, the data obtained with 2-butanone and 3-pentanone (Tables 2 and 3, respectively) pointed out that these molecules undergo dehydration reactions to a significant extent. Dehydration reactions probably also involve alcohol molecules in the case of 2-butanone and 3-pentanone flow experiments. Indeed secondary alcohols have been detected only in minor amounts due to thermodynamic constraints, but rapid hydrogenation/dehydrogenation equilibrium is likely established on the catalyst surface so that alcohol molecules are always available for consecutive reactions. Besides, TPSR data provide further evidence for the occurrence of dehydration reactions: indeed propylene and water were observed to desorb during TPSR of 1-propanol and *n*-propanal (Fig. 1 and 2). Also, a dehydration step is involved in the formation of 2-methyl-2-pentenal from the corresponding aldol intermediate.

Bowker *et al.* (*34*) explained the formation of olefins during 1-propanol and 1-butanol TPD from ZnO by invoking a dehydration mechanism based on abstraction of β-hydrogen atom (H^+) from an alkoxide species. Accordingly, abstraction is easier from a methyl group rather than from a methylene group, due to electronic factors. The same mechanism is likely to operate over the ZnCrO surface. As a matter of fact, results obtained during flow experiments (Tables 1, 2, and 3) indicated the following order of reactivity toward dehydration: 2-butanone (abstraction from one methyl and one methylene group) > 3-pentanone (abstraction from 2 methylene groups) > 1-propanol (abstraction from one methylene group). It can be concluded that a dehydrating function is effective over ZnCrO-based catalysts in spite of alkali addition: such a catalyst function operates essentially at the expense of 2-alkanols and secondary alcohols rather than of primary alcohols.

Dehydration may be partially responsible for the formation of hydrocarbons during HAS. In this respect it is worth noting that addition of alkali to unpromoted ZnCrO is effective in suppressing the production of ethers, whereas hydrocarbons are still produced although in minor amounts (*8, 30*).

Other Reactions

Decarboxylation

A decarboxylative step is expected to operate in ketonization reactions, which eventually results in the combined production of CO_2 and ketones.

The desorption of ethylene and CO_2 at high temperature in 1-propanol, *n*-propanal, and *n*-propanoic acid TPSR indicates that decarboxylation also operates in the formation of C_{N-1} olefins from C_N carboxylate species. Previous TPSR and IR investigations of linear and branched C_4 oxygenates (alcohols, aldehydes, and acids) provided evidence that olefins originate from carboxylate species under TPSR conditions (*24, 25, 27*). This function may account at least partially for the formation of hydrocarbons during HAS conditions.

Water–Gas Shift Reaction

The presence of CO among reaction products is explained by considering the occurrence of the water–gas shift reaction involving CO_2 and H_2.

Cracking Reactions

The formation of methane and of light hydrocarbons in TPSR and flow-microreactor experiments may be explained by cracking of heavier intermediates formed on the catalyst surface. As a matter of fact the catalyst discharged at the end of TPSR and flow-microreactor experiments was partially fouled, as indicated by its blackish color.

CONCLUSIONS

A number of chemical functions of the K_2O-promoted ZnCrO catalyst have been identified by the TPSR study of 1-propanol, *n*-propanal, and *n*-propanoic acid, including hydrogenation–dehydrogenation, normal and reversal aldolic-type condensations, ketonizations, reversal α-addition, dehydration, decarboxylation, and cracking. This corroborates and generalizes most of our previous conclusions based on TPSR experiments of C_4 oxygenates over the same catalytic system and provides additional evidence for reversal α-addition which was not discussed in details previously. On comparing these data with those obtained during flow experiments of 1-propanol, 3-pentanone, and 2-butanone at atmospheric pressure a strict correspondence is observed between the chemical functions revealed by the TPSR study and those operating at steady-state conditions. However, under these conditions some of the associated chemical reactions appear to be limited by chemical equilibria; in addition, the different reactivity of the species participating in the numerous chemical reactions can be appreciated.

Both TPSR and continuous-flow experiments converge in identifying a general reaction network for the chain growth to higher oxygenates, based on the following routes:

(1) Crossed aldolic-type condensations of aldehydes and ketones, which proceed in both the normal and the reversal modes. Higher aldehydes are produced in the first case and ketones are produced in the latter during condensations of two aldehydes; condensations involving ketones always result in the formation of higher ketones. Only aldehydes (linear and branched) participate in aldolic-type condensation reactions as electrophilic molecules. Both linear C_{2+} aldehydes and linear ketones can be involved as nucleophilic species, aldehydes showing higher reactivity than ketones. Branching in the two position reduces the reactivity of electrophilic reagents and prevents the participation of both aldehydes and ketones as nucleophilic species in aldolic-type condensations.

(2) Ketonization reactions, involving aldehydic or carboxylate surface species and leading to the formation of ketones and CO_2. Also in this case the presence of substituents in the α-position with respect to the carbonyl group hinders the reactivity of the reagents.

(3) Reversal α-addition reactions, which

involve the participation of aldehydic molecules and of a C_1 nucleophilic species and lead to the formation of 2-ketones. C_1 species are believed to be associated with nucleophilic oxygenated C_1 species originated during decarboxylation reactions.

Under flow-microreactor conditions, normal aldolic-type condensations and ketonization reactions dominate the chain growth mechanism at low temperatures (360°C), whereas at higher-temperature ketonization, reversal aldolic-type condensation and reversal α-addition are responsible for the formation of remarkable amounts of higher ketones.

It is worth noting that almost the same chemical functions have been invoked by Elliott and Pennella (*17*) to explain the product distribution obtained by passing 1-propanol over a CuO/ZnO-based catalyst at atmospheric pressure. However reversal α-addition has not been reported, and significant amounts of esters have been detected. As previously discussed, this is possibly related both to the lower temperature used in this case (285°C) and to the lack of the alkali promoter on the catalyst. These results eventually indicate that the chemistry involved in the formation of higher oxygenates over both low-*T* Cu-based catalysts and high-*T* ZnO/CrO catalysts is basically the same.

In addition to the chain growth mechanism reported above, oxygenates are also involved in the following reactions:

(1) Hydrogenation equilibria involving primary alcohols/aldehydes and secondary alcohols/ketones pairs. The signs of the deviations from chemical equilibrium observed at low temperatures indicate that carbonyl compounds are intermediates in the chain growth process whereas alcohols are produced by subsequent hydrogenations;

(2) Dehydration of oxygenates, and particularly of secondary alcohols, leading to the formation of olefins. Olefins may also be formed to a certain extent by decarboxylation of surface carboxylate species.

On comparing the reaction pattern identified in the present study with information obtained by catalytic activity tests and chemical enrichment experiments performed with various oxygenates under real synthesis conditions (*10, 25, 27, 36*), a strict correspondence is noted between the characteristic chemical functions revealed by the TPSR and flow-microreactor data and those determining the product distribution observed in HAS. This indicates that the reaction network of Fig. 4 is adequate to describe the reactions occurring under pressure as well. However, due to the different operating conditions, in the synthesis the relevance of some of the characteristic reactions is limited by chemical equilibria so that the concentration of related compounds are eventually very small. This is, for example, the case of ketonization reactions, which occur to a large extent during TPSR and flow experiments but are strongly depressed under pressure, and of hydrogenation reactions of aldehydes and ketones to the corresponding alcohols. The reaction network reported in Fig. 4 has provided the basis for the development of a mechanistic kinetic model for the distribution of C_{2+} oxygenate products in the HAS, which can account quantitatively for over 50 compounds in the reaction product mixture as function of contact time, temperature, pressure, and feed composition.

ACKNOWLEDGMENT

This work was supported by CNR–Progetto Finalizzato Chimica Fine 2 (Roma).

REFERENCES

1. Smith, K. J., and Anderson, R. B., *Can. J. Chem. Eng.* **61,** 40 (1983).
2. Klier, K., *in* "Catalysis on the Energy Scene" (S. Kaliaguine and A. Mahay, Eds.), p. 439. Elsevier, Amsterdam, 1984.
3. Vedage, G. A., Himelfarb, P. B., Simmons, G. W., and Klier, K., *ACS Symp. Ser.* **279,** 295 (1985).
4. Fornasari, F., Gusi, S., La Torretta, T. M. G., Trifirò, F., and Vaccari, A., *in* "Catalysis and Au-

tomotive Pollution Control" (A. Cruq and A. Frenuet, Eds.), p. 469. Elsevier, Amsterdam, 1987.
5. Nunan, J. G., Bogdan, C. E., Klier, K., Smith, K. J., Young, C. W., and Herman, R. G., *J. Catal.* **116,** 195 (1989).
6. Runge, F., and Zepf, K., *Brennstoff-Chem.* **35,** 167 (1954).
7. Riva, A., Trifirò, F., Vaccari, A., Busca, G., Mintchev, L., Sanfilippo, D., and Manzatti, W., *Chem. Soc., Faraday Trans. 1* **83,** 2213 (1987).
8. Tronconi, E., Ferlazzo, N., Forzatti, P., and Pasquon, I., *Ind. Eng. Chem. Res.* **26,** 2122 (1987).
9. Forzatti, P., Cristiani, C., Ferlazzo, N., Lietti, L., Pasquon, I., Tronconi, E., Villa, P. L., Antonelli, G. B., Sanfilippo, D., and Contarini, S., *in* "Actas 11th Iberoamerican Symposium on Catalysis" (F. Cossio, O. Bermudez, G. del Angel, and R. Gomez, Eds.), Vol. 2, p. 671. Guanajuato, Mexico, 1988.
10. Tronconi, E., Lietti, L., Forzatti, P., and Pasquon, I., *Appl. Catal.* **47,** 317 (1989).
11. Forzatti, P., Cristiani, C., Ferlazzo, N., Lietti, L., Tronconi, E., Villa, P. L., and Pasquon, I., *J. Catal.* **111,** 120 (1988).
12. Nunan, J. G., Bogdan, C. E., Klier, K., Smith, K. J., Young, C. W., and Herman, R. G., *J. Catal.* **113,** 410 (1988).
13. Smith, K. J., Herman, R. G., and Klier, K., *Chem. Eng. Sci.* **45,** 2639 (1990).
14. Klier, K., Herman, R. G., Nunan, J. G., Smith, K. J., Bogdan, C. E., Young, C. W., and Sebastian, J. G., *in* "Methane Conversion" (D. M. Bibby, C. D. Chang, R. F. Howe, and S. Yurchok, Eds.), p. 109. Elsevier, Amsterdam, 1988.
15. Elliott, D. J., and Pennella, F., *J. Catal.* **114,** 90 (1988).
16. Elliott, D. J., *J. Catal.* **111,** 445 (1988).
17. Elliott, D. J., and Pennella, F., *J. Catal.* **119,** 359 (1989).
18. Elliott, D. J., and Pennella, F., *J. Catal.* **102,** 464 (1986).
19. Natta, G., Colombo, U., and Pasquon, I., *in* "Catalysis" (P. H. Emmett, Ed.), Vol. 5. Reinhold, New York, 1957.
20. Frolich, K., and Cryder, S., *Ind. Eng. Chem.* **23,** 1051 (1930).
21. Graves, G. D., *Ind. Eng. Chem.* **23,** 1381 (1931).
22. Morgan, G. T., *Proc. R. Soc. A* **127,** 246 (1930).
23. Morgan, G. T., Douglas, D. V. N., and Proctor, R. A., *J. Chem. Soc. Chem. Ind. (London)* **41,** 1T (1932).
24. Lietti, L., Tronconi, E., and Forzatti, P., *J. Mol. Catal.* **44,** 201 (1987).
25. Lietti, L., Botta, D., Forzatti, P., Mantica, E., Tronconi, E., and Pasquon, I., *J. Catal.* **111,** 360 (1988).
26. Lietti, L., Tronconi, E., Forzatti, P., and Pasquon, I., *in* "Structure and Reactivity of Surfaces" (A. Zecchina, G. Costa, and C. Morterra, Eds.), p. 581. Elsevier, Amsterdam, 1989.
27. Lietti, L., Forzatti, P., Tronconi, E., and Pasquon, I., *J. Catal.* **126,** 401 (1990).
28. Lietti, L., Tronconi, E., Forzatti, P., and Busca, G., *J. Mol. Catal.* **55,** 43 (1989).
29. Tronconi, E., and Forzatti, P., *Chim. Ind. (Milan)* **70,** 66 (1988).
30. Tronconi, E., Forzatti, P., and Pasquon, I., *J. Catal.* **124,** 376 (1990).
31. Unpublished results from our laboratories.
32. Sanfilippo, D., SNAMPROGETTI, personal communication.
33. Santiesteban, J. G., Bogdan, C. E., Herman, R. G., and Klier, K., *in* "Proceedings, 9th International Congress on Catalysis, Calgary, 1988" (M. J. Phillips and M. Ternan, Eds.), Vol. 2, p. 561. Chem. Institute of Canada, Ottawa, 1988.
34. Bowker, M., Petts, R. W., and Waugh, K. C., *J. Catal.* **99,** 53 (1986).
35. Manuscript in preparation.
36. Tronconi, E., Forzatti, P., Groppi, G., Lietti, L., and Sanfilippo, D., *in* "Recent Advances in Chemical Engineering" (D. N. Saraf and D. Kunzru, Eds.), p. 217. Tata McGraw–Hill, New Dehli, 1989.